

Doubly Resonant IR-UV Sum-Frequency Vibrational Spectroscopy on Molecular Chirality

M. A. Belkin and Y. R. Shen*

*Department of Physics, University of California, Berkeley, CA 94720, USA
and Materials Sciences Division, Lawrence Berkeley National Laboratory, Berkeley, California 94720, USA
(Received 30 June 2003; published 21 November 2003)*

We show theoretically and experimentally that for sum-frequency vibrational spectroscopy near electronic transitions, resonant enhancement of the chiral response can be much stronger than that of the achiral response. The doubly resonant spectrum selectively enhances the vibrational modes through their different electron-vibration couplings. The unusually strong resonant enhancement significantly improves sensitivity of chiral spectroscopy and allows detection of the chiral vibrational spectrum of a molecular monolayer for the first time.

DOI: 10.1103/PhysRevLett.91.213907

PACS numbers: 42.65.An, 33.55.Ad, 68.18.-g, 78.30.Cp

Being the basis of all living organisms, chiral molecules play a key role in chemistry, biology, and medicine. However, only a few spectroscopic techniques are available to probe molecular chirality. The most common ones are measurements of optical activity, circular dichroism (CD), and Raman optical activity (ROA). All of them rely on electric-dipole forbidden processes [1] and therefore are not sufficiently sensitive to detect chirality from molecular monolayers or thin films. Yet such studies are highly desirable, for example, for understanding the adsorption and the change of conformation of proteins at interfaces [2] and the separation of chiral compounds on chiral surfaces [3]. Recently, it was demonstrated that optical second-harmonic generation [4,5] and sum-frequency generation (SFG) [6–8] can be used to obtain chiral spectra of molecular systems. Sum-frequency vibrational spectroscopy (SFVS), in particular, can yield chiral vibrational spectra directly related to the molecular chiral structure. These processes are electric-dipole allowed and would have high sensitivity to detect chirality, but SFVS on several chiral systems has found a chiral response many orders of magnitude smaller than that from an ordinary electric-dipole SFG process [6].

It is known that the optical nonlinearity responsible for SFVS near a vibrational resonance is proportional to the product of infrared and Raman amplitudes for the vibrational mode. The chiral nonlinearity of a bulk liquid, specifically, is proportional to the antisymmetric part of the Raman tensor [6]. The latter is known to be much smaller than its symmetric counterpart at frequencies far from electronic resonances because of partial cancellation of contributions from different vibronic states [9]. As the sum frequency (SF) approaches electronic resonances, the cancellation becomes worse and the chiral SFVS response should experience additional enhancement on top of the usual resonant enhancement.

In this Letter, we present a theory that shows explicitly the very different resonant dispersions of chiral and achiral responses in SFVS. To test the theory, we have carried out doubly resonant (DR) SFVS measurements on a bulk

1,1'-bi-2-naphthol (BN) solution in acetone and a monolayer of BN on water. The experiment showed good qualitative agreement with the theory. The strongest resonant enhancement in a chiral spectrum is more than 10^5 as SF approaches the first electronic resonance of BN, in contrast to about a 10^2 enhancement in an achiral spectrum. The enhancement is different for different vibrational modes because of significant differences in their electron-vibration coupling strengths. The very strong resonant enhancement of the chiral response enables us to record the first chiral vibrational spectrum of a chiral monolayer, namely, a BN monolayer on water. This makes SFVS as a novel probe of molecular chirality much more attractive.

The SFG signal at $\omega = \omega_1 + \omega_2$ from a sample in transmission or reflection is given by [10]

$$S(\omega) \propto |\chi_{\text{eff}}^{(2)}|^2 I_1(\omega_1) I_2(\omega_2),$$

$$\vec{\chi}_{\text{eff}}^{(2)} = [\vec{F}(\omega) \cdot \hat{e}] \cdot \vec{\chi}^{(2)} : [\vec{F}(\omega_1) \cdot \hat{e}_1][\vec{F}(\omega_2) \cdot \hat{e}_2], \quad (1)$$

$$\vec{\chi}^{(2)} = \vec{\chi}_S^{(2)} + \vec{\chi}_B^{(2)} / i\Delta k_z, \quad \Delta k_z = k_z - k_{1z} - k_{2z},$$

where \vec{k}_i , \hat{e}_i , $I_i(\omega_i)$, and $\vec{F}(\omega_i)$ are the wave vector, polarization, intensity, and tensorial Fresnel transmission coefficient, respectively, for the wave at ω_i , $\vec{\chi}_S^{(2)}$ and $\vec{\chi}_B^{(2)}$ are the surface and bulk nonlinear susceptibilities, and Δk_z is the phase mismatch. In terms of the second-order molecular hyperpolarizability $\vec{\alpha}^{(2)}$ [11], for $\vec{\chi}_{B,S}^{(2)}$ we have

$$\vec{\chi}_{B,S}^{(2)} = \frac{N_{B,S} L_{B,S}}{\epsilon_0} \langle \vec{\alpha}^{(2)} \rangle, \quad (2)$$

where N_B and N_S are the bulk and surface molecular densities, respectively, $L_{B,S}$ is the corresponding local-field correction factor, and the angular brackets denote the orientational average. Under the electric-dipole approximation, $\vec{\chi}_B^{(2)}$ vanishes from the orientational average in an ordinary liquid but has a nonvanishing chiral element in a chiral liquid,

$$\begin{aligned}\chi_B^{\text{chiral}} &= \chi_{ijk}^{(2)} \cdot \epsilon_{ijk} = \frac{N_B}{\epsilon_0} \langle (\hat{i} \cdot \hat{\xi}) \alpha_{\xi\eta\zeta}^{(2)} (\hat{j} \cdot \hat{\eta}) (\hat{k} \cdot \hat{\xi}) \rangle \\ &= \frac{N_B}{6\epsilon_0} (\alpha_{\xi\eta\zeta}^{(2)} - \alpha_{\eta\xi\zeta}^{(2)} + \alpha_{\eta\zeta\xi}^{(2)} - \alpha_{\zeta\eta\xi}^{(2)} + \alpha_{\xi\zeta\eta}^{(2)} \\ &\quad - \alpha_{\xi\zeta\eta}^{(2)}),\end{aligned}\quad (3)$$

where ϵ_{ijk} is the Levi-Civita symbol.

At a surface or interface, $\chi_S^{(2)}$ possesses both chiral and achiral components. As shown in Ref. [6], the chiral components of $\chi_S^{(2)}$ and $\chi_B^{(2)}$ can be assessed in SFG by polarization combinations *SPP* (*S*, *P*, and *P* polarizations for the fields at ω , ω_1 , and ω_2 , respectively), *PSP*, and *PPS* and the achiral ones by *PPP*, *SPS*, *SSP*, and *PSS*.

The resonant dispersions of $\alpha^{(2)}$ and $\chi^{(2)}$ come from their microscopic expressions. With ω_2 near vibrational resonances, $\alpha_{\xi\eta\zeta}^{(2)}$ has the near-resonant expression [11]

$$\alpha_{\xi\eta\zeta}^{(2)} = \frac{1}{\hbar} \sum_i \left(M_{\xi\eta} \frac{\langle g, 1 | \mu_{\zeta} | g, 0 \rangle}{(\omega_2 - \omega_{g1-g0} + i\Gamma_{g1-g0})} \right)_i, \quad (4)$$

where the index *i* refers to the *i*th vibrational mode, $\vec{\mu}$ is the dipole operator, ω_{g1-g0} and Γ_{g1-g0} are the frequency and damping constant for the vibrational transition from $|g, 1\rangle$ to $|g, 0\rangle$ with *g* referring to the electronic ground state, 0 and 1 refer, respectively, to the ground and the first excited vibrational state of the *i*th mode, and $M_{\xi\eta}$ is the

anti-Stokes Raman tensor element for the transition $|g, 1\rangle \rightarrow |g, 0\rangle$ with

$$M_{\xi\eta} = \frac{1}{\hbar} \sum_{n \neq g; \delta} \left[\frac{\langle g, 0 | \mu_{\xi} | n, \delta \rangle \langle n, \delta | \mu_{\eta} | g, 1 \rangle}{(\omega - \omega_{n\delta-g0} + i\Gamma_{n\delta-g0})} - \frac{\langle g, 0 | \mu_{\eta} | n, \delta \rangle \langle n, \delta | \mu_{\xi} | g, 1 \rangle}{(\omega + \omega_{n\delta-g1} + i\Gamma_{n\delta-g1})} \right]. \quad (5)$$

Following the derivations in Ref. [12], we can obtain a more explicit expression for $M_{\xi\eta}$. It starts by including vibronic coupling and nonadiabatic correction as first-order perturbations in expressing $|n, \delta\rangle$:

$$|n, \delta\rangle = |n\rangle |\delta_n\rangle + \sum_{s \neq n} |s\rangle \sum_{\nu} \frac{|\nu_s\rangle \langle \nu_s | Q(\frac{\partial H}{\partial Q}) | n \rangle |\delta_n\rangle}{\hbar \omega_{n\delta-s\nu}}, \quad (6)$$

where $Q(\frac{\partial H}{\partial Q})$ is the operator for the first-order vibronic coupling with *H* being the molecular Hamiltonian and *Q* the vibrational normal coordinate. Assuming $|\omega - \omega_{n\delta-g0}| \ll |\omega + \omega_{n\delta-g1}|$, we can neglect the second term in Eq. (5) and find

$$M_{\xi\eta} = A_{\xi\eta} + B_{\xi\eta} \quad (7)$$

with

$$A_{\xi\eta} = \frac{1}{\hbar} \sum_{n \neq g; \delta} \frac{\mu_{ng}^{\xi} \mu_{ng}^{\eta} \langle 0_g | \delta_n \rangle \langle \delta_n | 1_g \rangle}{(\omega - \omega_{n\delta-g0} + i\Gamma_{n\delta-g0})}, \quad (8)$$

$$B_{\xi\eta} = \frac{1}{\hbar^2} \sum_{n \neq g; \delta} \sum_{s \neq n, g; \nu} \left[\frac{\mu_{ng}^{\xi} h_{ns} \mu_{sg}^{\eta} \langle 0_g | \delta_n \rangle \langle \delta_n | Q | \nu_s \rangle \langle \nu_s | 1_g \rangle}{\omega_{n\delta-s\nu} (\omega - \omega_{n\delta-g0} + i\Gamma_{n\delta-g0})} + \frac{\mu_{sg}^{\xi} h_{ns} \mu_{ng}^{\eta} \langle 0_g | \nu_s \rangle \langle \nu_s | Q | \delta_n \rangle \langle \delta_n | 1_g \rangle}{\omega_{n\delta-s\nu} (\omega - \omega_{n\delta-g0} + i\Gamma_{n\delta-g0})} \right], \quad (9)$$

where $\mu_{lm}^{\xi} \equiv \langle l | \mu_{\xi} | m \rangle$ and $h_{lm} \equiv \langle l | (\frac{\partial H}{\partial Q})_0 | m \rangle$ are assumed real [9]. Similar expressions are obtained in Refs. [13,14]. Here we have neglected, for simplicity, the vibronic coupling in the ground electronic state as it is typically smaller than the vibronic coupling in the excited electronic states by the ratio of about ω_{ns}/ω_{ng} . Since the shift in the equilibrium positions between the ground and *n*th excited electronic states is $\Delta \approx -2h_{nn}Q_{01}^2/(\hbar\omega_Q)$ [13], we have $\omega_Q \langle 0_g | 1_n \rangle = -\omega_Q \Delta / (2Q_{01}) = h_{nn}Q_{01}/\hbar$. Thus, to the first order, both terms in Eq. (7) depend linearly on vibronic couplings and are of the same order of magnitude.

It is seen from Eqs. (3) and (4) that only the antisymmetric part of $M_{\xi\eta}$, namely, $M_{\xi\eta}^{as} \equiv \frac{1}{2}(M_{\xi\eta} - M_{\eta\xi})$, contributes to χ_B^{chiral} . The symmetric part, $M_{\xi\eta}^s \equiv \frac{1}{2}(M_{\xi\eta} + M_{\eta\xi})$, on the other hand, contributes to the achiral hyperpolarizability [6]. The ω dispersions of chiral and achiral hyperpolarizability components are then governed by $M_{\xi\eta}^{as}$ and $M_{\xi\eta}^s$, respectively. For $M_{\xi\eta}^s$, knowing $\langle \delta_m | \delta_n \rangle \approx 1$, $\langle 0_g | 1_n \rangle = -\langle 0_n | 1_g \rangle$, terms with $\delta \geq 2$ are negligible, and assuming equal damping constants for all electronic transitions, from Eqs. (8) and (9) we have

$$A_{\xi\eta}^s = A_{\xi\eta} \approx \frac{1}{\hbar} \sum_{n \neq g} \frac{\mu_{ng}^{\xi} \mu_{ng}^{\eta} \omega_Q \langle 0_g | 1_n \rangle}{(\omega - \omega_{n0-g0} + i\Gamma_{n0-g0})(\omega - \omega_{n1-g0} + i\Gamma_{n1-g0})}, \quad (10)$$

where ω_Q is the vibrational frequency. For $B_{\xi\eta}^s$, a representative leading term is

$$B_{\xi\eta}^s = \frac{1}{2\hbar^2} \sum_{n \neq g} \sum_{s < n, \neq g} h_{ns} Q_{01} (\mu_{ng}^{\xi} \mu_{sg}^{\eta} + \mu_{ng}^{\eta} \mu_{sg}^{\xi}) \left[\frac{1}{(\omega - \omega_{n0-g0} + i\Gamma_{n0-g0})(\omega - \omega_{s1-g0} + i\Gamma_{s1-g0})} + \frac{1}{(\omega - \omega_{n1-g0} + i\Gamma_{n1-g0})(\omega - \omega_{s0-g0} + i\Gamma_{s0-g0})} \right]. \quad (11)$$

For $M_{\xi\eta}^{as}$, the $A_{\xi\eta}^{as}$ term vanishes, and a representative leading term of $B_{\xi\eta}^{as}$ appears as

$$B_{\xi\eta}^{as} = \frac{1}{2\hbar^2} \sum_{n \neq g} \sum_{s < n, \neq g} h_{ns} Q_{01} (\mu_{ng}^{\xi} \mu_{sg}^{\eta} - \mu_{ng}^{\eta} \mu_{sg}^{\xi}) \left[\frac{1}{(\omega - \omega_{n0-g0} + i\Gamma_{n0-g0})(\omega - \omega_{s1-g0} + i\Gamma_{s1-g0})} - \frac{1}{(\omega - \omega_{n1-g0} + i\Gamma_{n1-g0})(\omega - \omega_{s0-g0} + i\Gamma_{s0-g0})} \right]. \quad (12)$$

Sufficiently far away from resonance, the two terms in the brackets cancel each other to a large extent and $B_{\xi\eta}^{as}$ can be approximated by

$$B_{\xi\eta}^{as} = \frac{1}{2\hbar^2} \sum_{n \neq g} \sum_{s < n, \neq g} h_{ns} Q_{01} (\mu_{ng}^{\xi} \mu_{sg}^{\eta} - \mu_{ng}^{\eta} \mu_{sg}^{\xi}) \times \frac{\omega_Q \omega_{s0-n0}}{(\omega - \omega_{n0-g0})^2 (\omega - \omega_{s0-g0})^2}. \quad (13)$$

As ω approaches ω_{n0-g0} , the cancellation becomes increasingly poor and $|B_{\xi\eta}^{as}|$ increasingly large. If we assume equal strengths for $\mu_{ng}^{\xi} \mu_{ng}^{\eta}$ and $\frac{1}{2}(\mu_{ng}^{\xi} \mu_{sg}^{\eta} \pm \mu_{ng}^{\eta} \mu_{sg}^{\xi})$ and $h_{nn} \sim h_{ns}$, it can become comparable to $|A_{\xi\eta}^s|$ and $|B_{\xi\eta}^s|$ ($|B_{\xi\eta}^{as}| \sim |B_{\xi\eta}^s|$ and $|A_{\xi\eta}^s|$ is larger by ω_{s0-n0}/ω_Q).

To test the theoretical prediction, we have studied DR-SFVS from BN. Molecular structure and UV absorption spectrum of BN are shown in Fig. 1(a). The two peaks in the spectrum come from transitions to the two exciton states separated by 0.22 eV, which corresponds to $\hbar\omega_{s0-n0}$ in the above equations [8].

Our experimental arrangement [Fig. 1(b)] for DR-SFVS was similar to the SFVS setup described in Ref. [6] except that both infrared and visible input pulses were tunable with pulsewidth 20 ps, a repetition rate 20 Hz, and energies $\sim 75 \mu\text{J}$ for ω_1 and $\sim 30 \mu\text{J}$ for ω_2 . They were generated from a Nd:YAG laser-pumped optical parametric system. To study the dispersion of chiral DR-SFVS, we measured SF output in reflection from a solution of 0.46M R-BN or S-BN in acetone. In this case, the chiral bulk contribution from χ_B^{chiral} dominated as it was more than 100 times stronger than that from a well oriented full monolayer of BN on water. The vibrational spectra were obtained by scanning ω_2 over vibrational resonances of BN while having ω_1 simultaneously adjusted to keep $\omega = \omega_1 + \omega_2$ fixed. The measurements were repeated for different values of ω . The very strong double-resonance enhancement allowed us to obtain also the chiral vibrational spectrum of a BN monolayer on water.

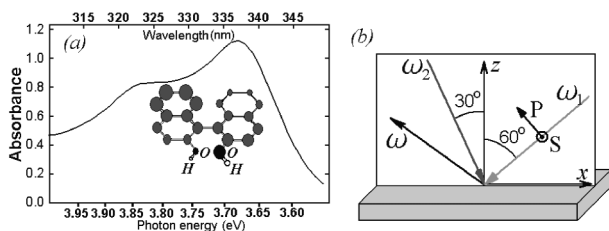


FIG. 1. (a) UV absorption spectrum of BN in acetone and the structure of the BN molecule. (b) Experimental geometry.

Figure 2(a) presents the representative SF chiral vibrational spectra at several sum frequencies ω obtained from the chiral BN solution in acetone using the *SPP* polarization combination. The absolute values of $|\chi_B^{\text{chiral}}/N_B|^2$ were deduced by calibrating against SFG from a crystalline quartz plate with $N_B = 2.8 \times 10^{26} \text{ m}^{-3}$. As seen in Fig. 2(a), there is a strong resonant enhancement as ω approaches the first excitonic resonance of BN at 3.67 eV. Compared to the spectrum taken at $\hbar\omega = 2.51 \text{ eV}$ far away from resonance, selected vibrational peaks in the spectrum taken at $\hbar\omega = 3.70 \text{ eV}$ experience an enhancement of more than 10^5 . For comparison, Fig. 2(b) displays the achiral vibrational spectra of $|\chi_{S,yyz}/N_S|^2$ (with $N_S = 2 \times 10^{18} \text{ m}^{-2}$ [8]) taken at the same set of ω values with the *SSP* polarization combination from a monolayer of BN on water (achiral elements of $\chi^{(2)}$ vanish in the bulk because of symmetry). The resonant enhancement is only ~ 200 . At the peak of resonance, $|\chi_{S,yyz}/N_S|$ is about 2.5 times larger than $|\chi_B^{\text{chiral}}/N_B|$.

The vibrational modes of BN in the 1300–1600 cm^{-1} range originate from *CH* bending and ring deformation modes. The *OH* bending modes may also show up in the 1350 cm^{-1} region [15]. A detailed assignment of the spectral peaks will have to come from a molecular dynamics calculation. Here, we only note that the observed SFVS spectra show very different resonant enhancements for different vibrational peaks. This is especially clear in the chiral SF spectra and is the result of very different vibronic couplings for different modes. Strong resonant enhancement, better assignment of modes through their

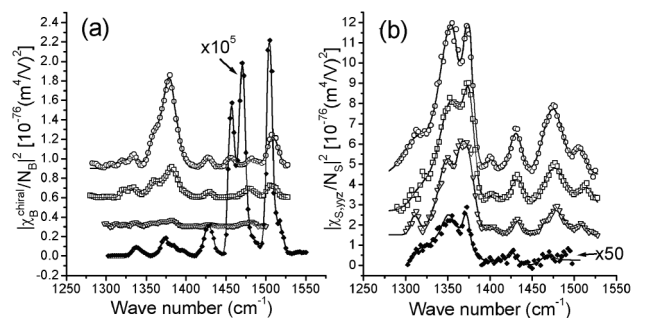


FIG. 2. (a) Chiral spectra $|\chi_B^{\text{chiral}}/N_B|^2$ of a 0.46M solution of R-BN in acetone and (b) achiral spectra $|\chi_{S,yyz}/N_S|^2$ of an R-BN monolayer on water with SF at 3.70 eV (open circles), 3.65 eV (open squares), 3.59 eV (open down triangles), and 2.51 eV (solid diamonds). The 2.51 eV spectra of $|\chi_B^{\text{chiral}}/N_B|^2$ and $|\chi_{S,yyz}/N_S|^2$ were multiplied by 10^5 and 50, respectively. Vertical shifts are used to separate spectra in the display and lines are for guiding the eye.

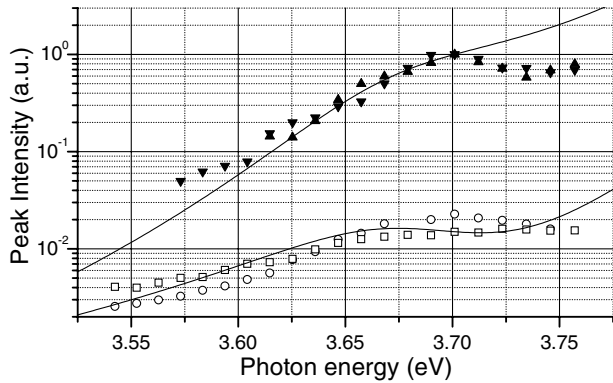


FIG. 3. Peak strengths of vibrational modes of BN at 1375 and 1430 cm^{-1} in $|\chi_{\text{chiral}}^{\text{bulk}}/N_B|^2$ (solid down and up triangles, respectively) and in $|\chi_{\text{S,yyz}}/N_S|^2$ (open squares and circles, respectively) versus $\hbar\omega$. Solid lines are calculated from the frequency dependence of $|B_{\xi\eta}^{\text{as}}|^2$ (upper curve) and $|B_{\xi\eta}^s|^2$ (lower curve) in Eqs. (12) and (11). Vertical shifts are used to separate spectra in the display.

selective resonant enhancement, and possible deduction of vibronic couplings for the modes are known to be the advantages of doubly resonant Raman spectroscopy. This is also the case for DR-SFVS but is exceptionally striking for chiral responses in DR-SFVS.

More detailed resonant enhancement behaviors of the 1375 and 1430 cm^{-1} vibrational modes near the first electronic resonance are shown in Fig. 3, where the peak intensities of $|\chi_B^{\text{chiral}}|^2$ and $|\chi_{\text{S,yyz}}|^2$ of the two vibrational modes are plotted against the sum-frequency ω . It is seen clearly that the chiral responses decrease much faster than the achiral ones as ω moves away from resonance. For theoretical comparison of this near-resonant case, we consider the BN molecule as a system with a vibrational mode at 1400 cm^{-1} and two exciton-split electronic excited states at 3.67 and 3.89 eV. The dependencies of $|\chi_B^{\text{chiral}}|$ and $|\chi_{\text{S,yyz}}|$ on ω are approximated by those of $M_{\xi\eta}^{\text{as}}$ and $M_{\xi\eta}^s$, and more crudely, by the resonant dispersions of $B_{\xi\eta}^{\text{as}}$ and $B_{\xi\eta}^s$, respectively, in Eqs. (11) and (12) or (13). From Fig. 3 one can see that these dispersions describe chiral and achiral experimental data quite well.

With the exceptionally strong resonant enhancement of the chiral response near double resonance, one would expect to be able to observe chiral vibrational spectra of a monolayer by SFVS. While achiral vibrational spectra of molecular monolayers are routinely measured, the chiral counterparts have never been observed before by any techniques. Using DR-SFVS on BN on water, we succeeded in recording the first chiral vibrational spectrum of a molecular monolayer. This is seen in Fig. 4, where it is also shown that no chiral spectral peaks are detectable from a monolayer of racemic mixture of BN. Because of the more ordered orientation of BN molecules adsorbed on water [8], the SPP spectrum appears different from the bulk one in the relative intensities of vibrational modes. Work is still needed to relate the spectra from SFVS to the molecular structure and orientation.

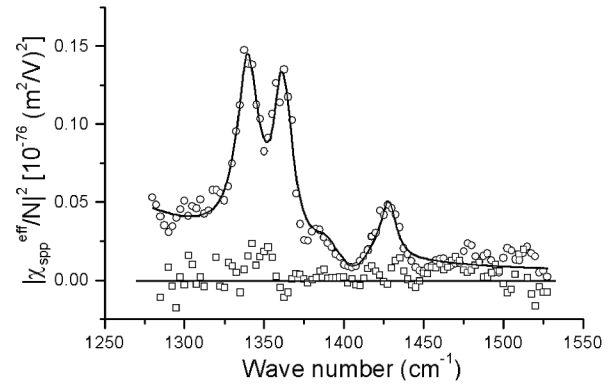


FIG. 4. SPP spectra of monolayers of R-BN (circles) and a racemic mixture of BN (squares) on water with SF at 3.70 eV.

In conclusion, we have demonstrated both theoretically and experimentally that vibrational-electronic double resonance can enhance the chiral SFVS spectra much more strongly than the achiral ones. Experimental results of DR-SFVS from a BN solution are in qualitative agreement with theoretical predictions. The exceptionally strong resonant enhancement makes detection of chiral vibrational spectra of molecular monolayers possible. Different vibrational modes show very different enhancements near an electronic resonance because of the different vibronic coupling strengths. This would facilitate assignment of modes in vibrational spectroscopic studies of chiral molecular structures.

This work was supported by the U.S. Department of Energy under Contract No. DE-AC03-76SF00098.

*Electronic address: shenyr@socrates.berkeley.edu

- [1] See, e.g., L. D. Barron, *Molecular Light Scattering and Optical Activity* (Cambridge University Press, Cambridge, UK, 1982).
- [2] See, e.g., S. Magdassi, *Surface Activity of Proteins: Chemical and Physicochemical Modifications* (Marcel Dekker, Inc., New York, 1996).
- [3] See, e.g., J. M. Bonello *et al.*, *J. Am. Chem. Soc.* **125**, 2723 (2003).
- [4] T. Petralli-Mallow *et al.*, *J. Phys. Chem.* **97**, 1383 (1993).
- [5] Jeffery J. Maki *et al.*, *Phys. Rev. B* **51**, 1425 (1995).
- [6] M. A. Belkin *et al.*, *Phys. Rev. Lett.* **85**, 4474 (2000).
- [7] M. A. Belkin *et al.*, *Phys. Rev. Lett.* **87**, 113001 (2001).
- [8] S.-H. Han *et al.*, *Phys. Rev. B* **66**, 165415 (2002).
- [9] F. Liu, *J. Phys. Chem.* **95**, 7180 (1991).
- [10] Y. R. Shen, *Annu. Rev. Phys. Chem.* **40**, 327 (1989).
- [11] Y. R. Shen, *The Principles of Nonlinear Optics* (J. Wiley, New York, 1984), Chap. 2.
- [12] F. Galluzzi, *Nuovo Cimento Soc. Ital. Fis.* **5D**, 100 (1985).
- [13] B. B. Johnson and W. L. Peticolas, *Annu. Rev. Phys. Chem.* **27**, 465 (1976).
- [14] B. B. Johnson *et al.*, *Chem. Phys.* **19**, 303 (1977).
- [15] V. Setnicka *et al.*, *J. Phys. Chem. A* **105**, 8931 (2001).